



HAL
open science

Retinal Phenotype of Patients with CLRN1-Associated Usher 3A Syndrome in French Light4Deaf Cohort

Vasily M Smirnov, Marco Nassisi, Saddek Mohand-Saïd, Crystel Bonnet, Anne Auboïs, Céline Devisme, Thilissa Dib, Christina Zeitz, Natalie Loundon, Sandrine Marlin, et al.

► **To cite this version:**

Vasily M Smirnov, Marco Nassisi, Saddek Mohand-Saïd, Crystel Bonnet, Anne Auboïs, et al.. Retinal Phenotype of Patients with CLRN1-Associated Usher 3A Syndrome in French Light4Deaf Cohort. Investigative Ophthalmology & Visual Science, 2022, 63 (4), pp.25. 10.1167/iovs.63.4.25 . hal-03954493

HAL Id: hal-03954493

<https://cnrs.hal.science/hal-03954493>

Submitted on 24 Jan 2023

HAL is a multi-disciplinary open access archive for the deposit and dissemination of scientific research documents, whether they are published or not. The documents may come from teaching and research institutions in France or abroad, or from public or private research centers.

L'archive ouverte pluridisciplinaire **HAL**, est destinée au dépôt et à la diffusion de documents scientifiques de niveau recherche, publiés ou non, émanant des établissements d'enseignement et de recherche français ou étrangers, des laboratoires publics ou privés.



Distributed under a Creative Commons Attribution 4.0 International License

Retinal Phenotype of Patients with *CLRN1*-Associated Usher 3A Syndrome in French Light4Deaf Cohort

Vasily M. Smirnov,^{1,2} Marco Nassisi,¹ Saddek Mohand-Saïd,^{1,3} Crystel Bonnet,⁴⁻⁶ Anne Auboïs,³ Céline Devisme,³ Thilissa Dib,³ Christina Zeitz,¹ Natalie Loundon,^{7,8} Sandrine Marlin,⁸ Christine Petit,^{4-6,9} Bahram Bodaghi,¹⁰ José-Alain Sahel,^{1,3,11-13} and Isabelle Audo^{1,3,14}

¹Sorbonne Université, INSERM, CNRS, Institut de la Vision, Paris, France

²Université de Lille, Faculté de Médecine, Lille, France

³CHNO des Quinze-Vingts, Centre de Référence Maladies Rares REFERET and DHU Sight Restore, INSERM-DGOS CIC1423, Paris, France

⁴Unité de Génétique et Physiologie de l'Audition, Institut Pasteur, Paris, France

⁵Unité Mixte de Recherche en Santé 1120, INSERM, Paris, France

⁶Institut de l'Audition, Paris, France

⁷Otorhinolaryngologie Pédiatrique, APHP Hôpital Necker, Paris, France

⁸Centre de référence des Surdités Génétiques, Service de Génétique, APHP Hôpital Necker, Paris, France

⁹Collège de France, Paris, France

¹⁰Hôpital Pitié-Salpêtrière, Paris, France

¹¹Fondation Ophthalmologique Adolphe de Rothschild, Paris, France

¹²Department of Ophthalmology, University of Pittsburgh Medical School, Pittsburgh, Pennsylvania, United States

¹³Académie des Sciences-Institut de France, Paris, France

¹⁴Institute of Ophthalmology, University College of London, London, United Kingdom

Correspondence: Isabelle Audo, 17, Rue Moreau, 75012 Paris, France; isabelle.audo@inserm.fr.

Received: November 28, 2020

Accepted: April 7, 2022

Published: April 28, 2022

Citation: Smirnov VM, Nassisi M, Mohand-Saïd S, et al. Retinal phenotype of patients with *CLRN1*-associated Usher 3A syndrome in French Light4Deaf cohort. *Invest Ophthalmol Vis Sci.* 2022;63(4):25. <https://doi.org/10.1167/iovs.63.4.25>

PURPOSE. Biallelic variants in *CLRN1* are responsible for Usher syndrome 3A and non-syndromic rod-cone dystrophy (RCD). Retinal findings in Usher syndrome 3A have not been well defined. We report the detailed phenotypic description of RCD associated with *CLRN1* variants in a prospective cohort.

METHODS. Patients were clinically investigated at the National Reference Center for rare ocular diseases at the Quinze-Vingts Hospital, Paris, France. Best-corrected visual acuity (BCVA) tests, Goldmann perimetry, full-field electroretinography (ffERG), retinal photography, near-infrared reflectance, short-wavelength and near-infrared autofluorescence, and optical coherence tomography (OCT) were performed for all patients.

RESULTS. Four patients from four unrelated families were recruited. Mean follow-up was 11 years for three patients, and only baseline data were available for one subject. Median BCVA at baseline was 0.2 logMAR (range, 0.3–0). ffERG responses were undetectable in all subjects. The III4e isopter of the Goldmann visual field was constricted to 10°. The retinal phenotype was consistent in all patients: small whitish granular atrophic areas were organized in a network pattern around the macula and in the midperiphery. OCT showed intraretinal microcysts in all patients. Upon follow-up, all patients experienced a progressive BCVA loss and further visual field constriction. Four distinct pathogenic variants were identified in our patients: two missense (c.144T>G, p.(Asn48Lys) and c.368C>A, p.(Ala123Asp)) and two frameshift variants (c.176del, p.(Gly59Valfs*13) and c.230dup, p.(Ala78Serfs*52)).

CONCLUSIONS. RCD in Usher 3A syndrome has some distinctive features. It is a severe photoreceptor dystrophy with whitish granular posterior pole appearance and cystic maculopathy.

Keywords: Usher 3 syndrome, retinal degeneration, natural history

Usher syndrome (USH) is the leading genetic cause of deafness and blindness and is inherited as an autosomal recessive trait. Its prevalence is estimated at 3 to 6 per 100,000.¹⁻⁴ USH is a clinically heterogeneous group of disorders with three main reported clinical subtypes associ-

ated with variable severity of deafness, vestibular dysfunction, and rod-cone dystrophy (RCD), a form of retinitis pigmentosa (RP).⁵ Usher syndrome type 1 (USH1), the most severe form of USH, includes bilateral profound congenital sensorineural hearing loss (SNHL), vestibular dysfunction,

and RCD. Pathogenic variants in *MYO7A* (MIM *276903), encoding myosin VIIA, an unconventional myosin linked with intracellular movement,⁶ are the most common cause of USH1 and are responsible not only for USH1B (MIM #276900) but also for non-syndromic SNHL.⁷

Usher syndrome type 2 (USH2) is characterized by RCD and variable severity (mild to severe) of congenital SNHL without vestibular dysfunction.⁸ Biallelic variants in *USH2A* (MIM *608400), encoding usherin, a protein involved in periciliary membrane complex in photoreceptors and in interstereocilia ankle in the inner ear sensory cells,⁹ are the leading cause of USH2 (underlying USH2A, MIM #276901)¹⁰ and are also responsible for non-syndromic autosomal recessive RCD (RP39, MIM #613809).^{11–13}

Usher syndrome type 3 (USH3) was defined on the basis of audiological features in the 1970 and 1980s.^{1,4,15} It is characterized by progressive postlingual SNHL and variable (none to progressive) vestibular dysfunction. Language and motor development are normal in most subjects. Onset of progressive SNHL begins in the first decade of life. About 50% of patients are profoundly deaf by their 40s.¹⁶

Pathogenic variants in two genes have been associated with USH3: *CLRN1* (MIM *606397), which encodes clarin-1, a four transmembrane-domain protein with a possible role in sensory synapses¹⁷ (involved in USH3A, MIM #276902), and *HARS1* (MIM *142810), encoding histidyl-tRNA synthetase 1, catalyzing the ligation of histidine to its cognate tRNA¹⁸ (involved in USH3B, MIM #614504). Biallelic variants in *CLRN1* have also been reported in non-syndromic RCD (RP61, MIM #614180).¹⁹ Patients with *HARS1* variants are rare, and all present syndromic manifestations including cochleo-vestibular involvement,²⁰ axonal peripheral neuropathy consistent with Charcot-Marie-Tooth 2W syndrome (MIM #616625),^{21,22} and/or ataxia.²³

USH3A associated with *CLRN1* mutations is uncommon. It represents only 2% of all patients with Usher syndromes in non-Finnish European populations,²⁴ but it causes 40% to 45% of the Usher cases in Finland.²⁵ The most common pathogenic variant in the Finnish population is c.528 T>G, p.(Tyr176*), suggesting a founder effect. USH3A is also more common (about 10% of the Usher patients) in Israeli and Palestinian populations.²⁶ A founder pathogenic variant of *CLRN1* is also reported in Ashkenazi Jews (c.144T>G, p.(Asn48Lys)).^{27,28}

There are only a few reports describing the ophthalmological features of *CLRN1*-related USH3A due to the rarity of this disorder. A large study cohort that included 90 Finnish patients demonstrated that the clinical course of *CLRN1*-related syndromic RCD due to the founder variant c.528 T>G, p.(Tyr176*) was similar to that for USH1 and USH2 individuals with non-specific retinal imaging findings.²⁵ In a series of 10 non-Finnish USH3A patients, RCD was more severe and rapidly progressive compared to patients harboring *USH2A* gene defects.²⁹ The cone mosaic assessed by adaptive optics was normal within the four central retinal degrees with spared ellipsoid zone (EZ) in three USH3A patients.³⁰ In Ashkenazi Jewish patients harboring the c.144T>G, p.(Asn48Lys) founder pathogenic *CLRN1* variant, night blindness and visual field constriction appeared early in life (early childhood to late teens) in one third of patients prior to the auditory symptoms. One third of patients were legally blind (i.e., below 1.3 logMAR) by their 50s.²⁸

The aim of our study was to report the retinal phenotype of a series of French patients with *CLRN1*-related USH3A

and to compare it with previously reported European and Israeli/Palestinian cohorts.

PATIENTS AND METHODS

Clinical Investigation

Patients with a molecular diagnosis of USH were included in a large prospective cohort study of USH syndromes (Light4Deaf, NCT04665726, www.clinicaltrials.gov). Patients were clinically investigated at the National Reference Center for Rare Retinal Diseases of Quinze-Vingts Hospital, Paris, France. Ophthalmic examination was performed as previously described.³¹ Prior to testing, written informed consent, approved by the Comité de Protection des Personnes, was obtained from each study participant or their parents. The study protocol adhered to the tenets of the Declaration of Helsinki and was approved by the local ethics committee. The study was performed in compliance with Oviedo Convention and Treaty of Lisbon.

Genetic Analysis

For most patients, a multiplex amplicon panel (Fluidigm Access Array; Fluidigm Corporate, San Francisco, CA, USA) was applied as previously described²⁴ to analyze all coding and noncoding exons of the 10 USH genes: *MYO7A*, myosin VIIA (MIM #276903); *USH1C*, harmonin (MIM #605242); *CDH23*, cadherin 23 (MIM #605516); *PCDH15*, protocadherin 15 (MIM #605514); *USH1G*, sans (MIM #607696); *CIB2*, calcium- and integrin-binding 2 (MIM #605564); *USH2A*, usherin (MIM #608400); *ADGRV1*, adhesion G protein-coupled receptor V1 (MIM #602851); *WHRN*, whirlin (MIM #607928); *CLRN1*, clarin-1 (MIM #606397); and the USH2 modifier gene *PDZD7*, PZD domain-containing 7 (MIM #612971). For some individuals, direct Sanger sequencing of coding sequences and flanking intronic regions of *CLRN1* were performed.^{27,32} Family segregation of the identified variants was performed when possible. All patients harboring biallelic pathogenic variants in *CLRN1* were subsequently included in this study.

Clinical Data Collection

Clinical data were retrospectively collected from medical records. These included sex, age at time of diagnosis and examination, personal or family history, symptoms, best-corrected visual acuity (BCVA) assessed by the Early Treatment Diabetic Retinopathy Study (ETDRS) chart, refractive errors, slit-lamp biomicroscopy, Lanthony D-15 panel, Goldmann kinetic visual fields (VFs; Haag-Streit, Koeniz, Switzerland), full-field electroretinogram (ffERG; ColorDome, Diagnosys, Cambridge, UK), spectral-domain optical coherence tomography (SD-OCT), fundus photography, and short-wavelength fundus autofluorescence (SWAF) and near-infrared fundus autofluorescence (NIRAF) imaging (SPECTRALIS HRA-OCT; Heidelberg Engineering, Heidelberg, Germany). Structural changes were evaluated using Heidelberg Eye Explorer, version 1.9.10.0 (Heidelberg Engineering). We measured the horizontal and vertical diameters of the remaining central retina on three retinal imaging modalities: first, the preserved ellipsoid zone on SD-OCT scans passing through the fovea; second, the ring of increased autofluorescence on SWAF (SWAF-RIA); and, third, the area of preserved autofluorescence on NIRAF (NIRAF-

APA). For SD-OCT, the follow-up setting for horizontal and vertical images was used to ensure consistent measurements in serial images.

Statistical Analysis

Statistical analyses were performed using SPSS Statistics 21.0 (IBM, Chicago, IL, USA), with $P \leq 0.05$ considered statistically significant.

We applied the Wilcoxon signed-rank test for BCVA, NIRAF-APA, and EZ diameters to evaluate the agreement between eyes. We then averaged the two values for further analyses. The rate of annual progression for NIRAF-APA and EZ diameters was calculated as follows: (value on first visit – value on last visit)/(years of follow-up).

RESULTS

We identified four patients (two males and two females) with *CLRN1*-related USH3A in our Usher database comprised of 289 index patients in total, leading to a prevalence of 1.4% in our USH cohort. Three families were of African ancestry: F65 (CIC00088) from Algeria, F196 (CIC03005), and F2792 (CIC05477) from Ivory Coast. F937 (CIC02644) was of Ashkenazi Jewish descent.

The clinical data at first assessment are summarized in Table 1. Night blindness was the first symptom of disease, appearing at 10 to 12 years of age in all patients. The mean age at the initial examination was 18.5 years. The mean BCVA was 0.2 ± 0.08 logMAR. The Goldmann visual field at the III4e/V4e target was severely constricted in all patients. Subjects CIC03005 and CIC05477 had a residual temporal peripheral crescent of visual field at V4e target. Static perimetry showed a ring-shaped scotoma with variable preservation of foveal threshold. Color vision tests showed normal results (CIC02644), multiple without-axis errors (CIC00088 and CIC05477), or tritan axis dyschromatopsia (CIC03005). Full-field ERG was undetectable in all patients.

At slit-lamp examination, patients CIC00088 and CIC02644 had a posterior subcapsular cataract in each eye. Multimodal retinal imaging is presented in Figure 1. Fundus findings were typical of severe RP: waxy pallor of the optic disc, retinal vasculature narrowing, and pigmentary changes (Figs. 1A–1D). However, all patients presented an unusual whitish granularity of the midperipheral retina as a distinctive feature (Figs. 1A–1D, Supplementary Fig. S1). SWAF, NIRAF, and SD-OCT findings were typical of RP.

Long-term follow-up data were available for three patients (Table 2, Figs. 1A–1D, Figs. 2A–2C). BCVA was stable until 25 years of age and then gradually decreased (Fig. 2A). The peripheral visual field rapidly became constricted with relative preservation of central vision (Table 2). EZ and NIRAF-APA diameters decreased altogether but not completely in parallel (Figs. 2B, 2C). Cystic macular changes were observed in all patients on initial examination. Patient CIC05477 was assessed only once at 19 years of age. Unfortunately, the patient did not return for follow-up visits.

We identified four *CLRN1* variants (Fig. 3A, Supplementary Table S2): one duplication (c.230dup, p.(Ala78Serfs*52)²⁴); one deletion (c.176del, p.(Gly59Valfs*13)²⁴); and two missense (c.368C>A, p.(Ala123Asp)³³ and c.144T>G, p.(Asn48Lys)).¹⁷ All variants had been previously reported and were classified as pathogenic according to the

American College of Medical Genetics and Genomics guidelines.³⁴ Patient CIC02644 (Ashkenazi Jewish) was a compound heterozygous for c.176del, p.(Gly59Valfs*13) and c.144T>G, p.(Asn48Lys), the latter being a founder.^{23,24} The remaining three patients carried homozygous changes: patient CIC00088 carried the homozygous duplication (c.230dup, p.(Ala78Serfs*52)), whereas the other two patients (CIC03005 and CIC05477) carried the homozygous missense variant (c.368C>A, p.(Ala123Asp)). Two patients reported a history of parental consanguinity (CIC00088 and CIC05477). Parents of CIC03005 were born in the same village from Ivory Coast, but there was no identifiable parental consanguinity (Fig. 3B).

ENT data are summarized in the Table 1 but are beyond the scope of this study. Because the auditory and vestibular phenotype of patients harboring the aforementioned variants have already been reported, our study focused on the first documentation of retinal findings.

DISCUSSION

CLRN1-related USH3A is relatively rare in non-Finnish European populations. It accounts for 1.4% of our cohort of Usher patients. At present, there are only a few reports of audiological^{15,16,35} and retinal^{25,29,30} phenotypes in USH3A.

On initial examination, the RCD was severe in our patients. Despite a relatively preserved visual acuity, all patients had abnormal color vision with tritan or anarchic color vision defects. Visual field was severely constricted from the teen years; if initially present, the remaining temporal crescent disappeared within a decade on Goldmann perimetry. None of the studied patients had detectable fERG responses at presentation in their teen years.

The functional data of our patients were similar to those of previously reported series.^{25,28,29,36} In the largest USH3A ocular phenotype study of Finnish patients harboring the founder p.(Tyr176*) variant in *CLRN1*,²⁵ mean BCVA was 0.2 logMAR or better at 20 years of age, ranged from 0.2 to 0.6 logMAR at 30 years of age, and was equal or worse than 0.6 logMAR at 35 years. We observed the same rate of BCVA loss in our study (Fig. 2A). However, visual fields were more severely constricted in our patients, as two out of four had tubular fields without peripheral islands before 20 years of age, whereas in the Finnish cohort a similar stage was reached at an age of 30 years. More recent reports^{29,36} compared the progression of the retinal disease in subject with *CLRN1*-related USH3A and *USH2A*-related USH2A. The authors²⁹ concluded that *CLRN1*-associated retinal disease was more severe at a given age and was more rapidly progressing than *USH2A*-associated RCD.

The severity of retinal dysfunction in our cohort was mirrored by structural alterations. Only a small foveal island of outer retina was preserved. SWAF-RIA in the posterior pole was present at the initial visit in two of the four subjects (CIC00088 and CIC05477). It was faint and rapidly replaced by patches of hypo-autofluorescence due to rapid outer retinal atrophy. Poor outer retinal preservation was also apparent on the NIRAF imaging, with only a small remaining area of normal autofluorescence that rapidly diminished (e.g., –107 $\mu\text{m}/\text{y}$ on average for CIC02644). NIRAF alterations have been reported to precede SWAF alterations and have been found to better correlate with SD-OCT findings in RP.^{37,38} Indeed, the borders of NIRAF-APA usually coincide with the relative preservation of the EZ on SD-OCT.³⁷ We recog-

TABLE 1. Initial Clinical Features of Patients with *CLRN1*-Related USH3A

Patient, Sex, Ancestry	Age at First Examination (y)	Symptoms	BCVA (logMAR) and Refraction		Anterior Segment	Fundus	SWAF	NIRAF	OCT	KP	SP MD/FT (RE/LE)	Color Vision	fERG	Remarks
			RE	LE										
CIC00088, M, Algerian	22	Hearing difficulties at 20 y; night blindness from 10 y	RE: 0.5; +1.50 (-1.25); 20° LE: 0.2; +1.50 (-1.25); 150°		Anterior polar cataract OU Cataract surgery at 34 y	Waxy disc pallor Vessel narrowing Whitish retina at posterior pole and whitish granularity of the midperipheral retina Bone spicules-like, paravascular pigmentary cuffs, coarse pigment clumps in midperiphery	Perifoveal RIA, patchy paramacular and midperipheral hypoAF	Small central APA	Small foveolar area of preserved EZ, outer retinal layers disorganization outside maculopathy ILM thickening and irregular retinal surface	III4e constricted to 5° OU	17.9/15 16.7/22	Severe defect without axis (RE) Normal (LE)	Undetectable	Audiogram: middle and high-frequency losses MD REar: -53 dB MD LEar: -49 dB Hearing aids from 20 y
CIC02644, F, Ashkenazi Jewish	16	Mild hearing loss at 5 y; night blindness at 12 y	RE: 0; +1.75 (-2.0); 45° LE: 0.1; +1.75 (-2.0); 135°		Posterior subcapsular opacities OU	Waxy disc pallor Vessel narrowing Normal aspect of the macula Midperipheral whitish granularity, spotted marble appearance Bone spicules, paravascular pigmentary cuffs, sparse pigmentary clumps in midperiphery	Narrow perifoveal RIA, patchy paramacular and midperipheral hypoAF, some punched-out AF loss in midperiphery	Small central APA	Foveal area of preserved EZ, disorganization of the outer retinal layers replaced by hyperreflective dots outside the fovea Microcystic maculopathy (in INL and OPL)	KP: III4e constricted to 10°	17.3/29 16.8/32	Normal (both eyes)	Undetectable	—

TABLE 1. Continued

Patient Sex, Ancestry	Age at First Examination (y)	Symptoms	BCVA (logMAR) and Refraction	Anterior Segment	Fundus	SWAF	NIRAF	OCT	KP	SP MD/FT (RE/LE)	Color Vision	fERG	Remarks
CIC03005, F Ivory Coast	17	Night blindness from 12 y	RE: 0.4; +3.0 (-0.75); 135° LE: 0.6; +2.0 (-0.75); 35°	Normal	Arteriolar narrowing Yellowish macula, microcystic maculopathy Whitish granularity of midperipheral retina, spotted marble appearance Bone spicule-like and paravascular pigmentary cuffs	SWAF: posterior pole globally hypoAF with foveolar hyperAF Patchy midperipheral hypoAF	Small central APA	Small foveolar area of preserved EZ, disorganized outer retinal layers outside the fovea Microcystic maculopathy ILM thickening and irregularity	V4e constricted to 60° + temporal crescent OU	18.8/15 24.3/12	Tritan defect (both eyes)	Undetectable	Seizures, valproate treatment
CIC05477, M, Ivory Coast	20	Progressive hearing loss starting at 7 y; night blindness at 10 y	RE: 0.1; +1.75 (-1.75); 15° LE: 0.2; +1.75 (-1.75); 170°	Normal	Arteriolar narrowing Normal aspect of the macula, midperipheral whitish granularity, spotted marble appearance Few bone spicule-like pigments in midperiphery	SWAF: well-circumscribed perifoveal RFA, patchy midperipheral hypoAF	Foveal APA	Foveal area of preserved EZ, disorganization of the outer retinal layers replaced by hyperreflective dots outside the foveal region Microcystic maculopathy (in INL and OPL)	KP: V4e constricted to 20° + temporal crescent OU	21.2/22 21.6/21	Multiple errors without axis (both eyes)	Undetectable	Audiogram: severe middle and high-frequency loss MD REar: -100 dB MD LEar: -75 dB Normal speech Hearing aids from 7 y; cochlear implant at 21 y

KP, kinetic perimetry; SP, static perimetry; MD, mean deficit; FT, foveal threshold (dB); M, male; F, female; RE, right eye; LE, left eye; OU, both eyes; hypoAF, hypo-autofluorescence; hyperAF, hyper-autofluorescence; APA, area of preserved autofluorescence; REar, right ear; LEar, left ear; INL, inner nuclear layer; OPL, outer plexiform layer; ILM, internal limiting membrane (dB).

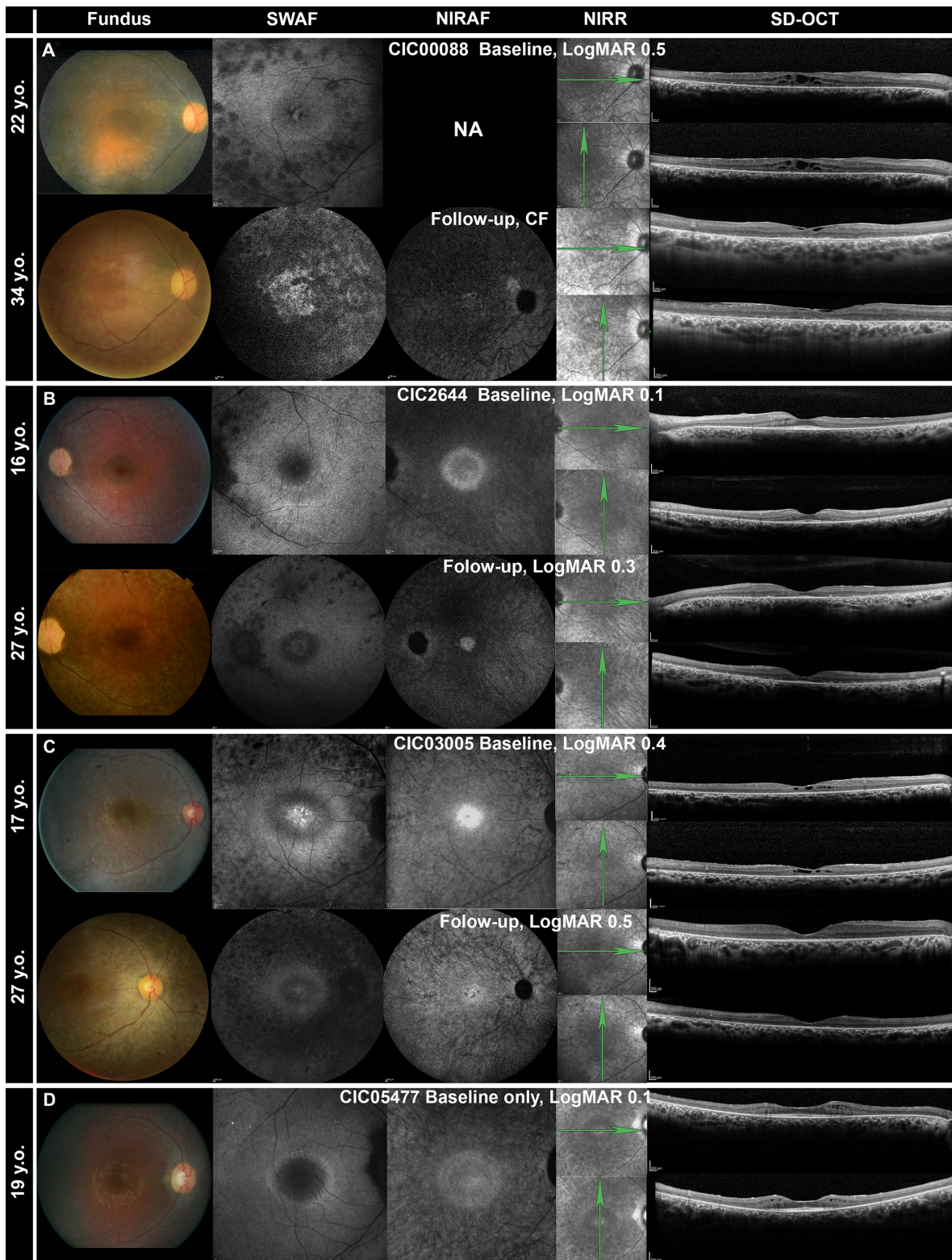


FIGURE 1. Multimodal retinal imaging in patients with *CLRN1* USH3A at first assessment and follow-up. Color fundus photography, SWAF, NIRAF, near-infrared reflectance (NIRR), and SD-OCT horizontal and vertical cross-section images. **(A)** Patient CIC00088, **(B)** Patient CIC2644, **(C)** Patient CIC03005, and **(D)** Patient CIC05477. All patients had classical signs of RP on fundus photography: optic disc pallor, arterial narrowing, and pigmentary changes. The distinctive feature was a granularity and whitishness of retina, present in all patients and prominent in CIC2644 and CIC03005. Only patient CIC05477 had a typical ring of increased autofluorescence on SWAF. The remaining cases show ill-defined perifoveal changes with hyper-autofluorescence (CIC03005) or iso-autofluorescence (CIC00088). On follow-up, hypo-autofluorescent zones increased. NIRAF showed a progressive narrowing of the area of preserved autofluorescence (APA) in the posterior pole, seen in CIC05477, where it was no longer present in patient CIC00088 at the last visit. Patient CIC03005 had some black dots in APA suggestive of foveal outer retinal disruption. SD-OCT revealed various degrees of outer nuclear layer, EZ, and RPE preservation. There were multiple hyperreflective dots in the subretinal space, especially in patients with prominent whitishness of the retina (CIC02644 and CIC03005). All patients had microcystic macular changes. Patient CIC00088 developed an epimacular membrane. CF, counting fingers.

TABLE 2. Longitudinal Follow-Up of Patients with *CLRN1*-Related USH3A

Patient	Follow-Up Period (y)	BCVA at Last Visit (logMAR), RE/LE; Age	Visual Field Progression	Color Vision at Last Visit	SWAF	NIRAF	OCT
CIC00088	12	CF/0.6; 34 y	Temporal crescents diminished and finally disappeared at the age 25. The central V4c isopter reduction was only of 5° over the 12 y.	Multiple without-axis errors appeared in RE, whereas the LE color vision remained unchanged.	RIA disappeared at age 25. Scalloped patches of midperipheral hypo-autofluorescence became larger and confluent, more advanced in the macular area (Fig. 1A).	APA disappearance at age 32 (Fig. 1A)	The EZ was preserved at the fovea at age 22 and disappeared at age 32 (Figs. 2B, 2C) Cystic maculopathy resolved at the same age. There was a thick epimacular membrane at the last visit (Fig. 1A). EZ was regularly decreasing for both the vertical (90 μm/y) and the horizontal (100 μm/y) diameters (Figs. 2B, 2C). Cystic macular changes appeared at 18 y and had been successfully treated by acetazolamide for 4 y. The treatment was then discontinued without recurrence of microcysts (Fig. 1B).
CIC02644	11	0.2/0.3; 27 y	Progressive loss and finally disappearance (at 24 y) of the temporal peripheral crescents The extent of the central V4c isopter did not change. Mean defect was slowly worsening, with a loss of 3 dB in the RE (-18%) and 2 dB in the LE (-12%) compared with the first assessment.	Color vision was first normal but a tritan defect became obvious.	RIA disappeared at 24 y and was replaced by a large ring of hypo-autofluorescence	APA was regularly decreasing for both the vertical (113 μm/y) and the horizontal (102 μm/y) diameters (Figs. 2B, 2C).	EZ was regularly decreasing for both the vertical (90 μm/y) and the horizontal (100 μm/y) diameters (Figs. 2B, 2C). Cystic macular changes appeared at 18 y and had been successfully treated by acetazolamide for 4 y. The treatment was then discontinued without recurrence of microcysts (Fig. 1B).
CIC03005	9	0.5/0.5; 30 y	Kinetic visual field was normal under the age of 20 y. Temporal peripheral crescents disappeared at 24 y, and the isopter V4c became constricted to 10° at 25 y.	A tritan color vision defect was present at the first assessment and remained unchanged.	Unchanged	Unchanged	The EZ was already disorganized on the first SD-OCT and remained unchanged Irregular-shaped macular microcysts persisted at all visits despite the acetazolamide treatment (Fig. 1C)

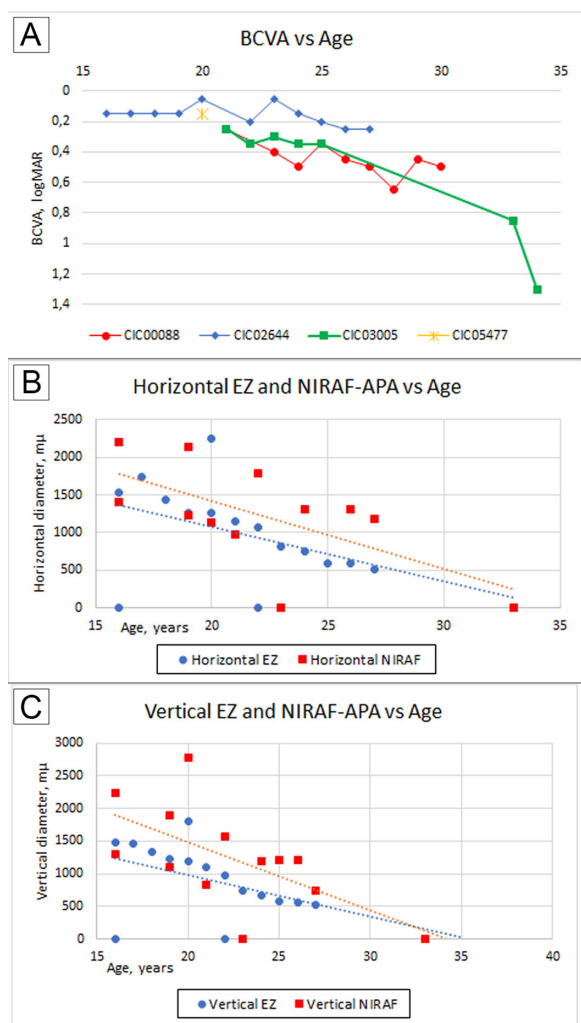


FIGURE 2. Longitudinal follow-up. (A) BCVA changes. (B) Horizontal EZ and NIRAF-APA changes. (C) Vertical EZ and NIRAF-APA changes.

nize, however, the difficulty of obtaining reliable NIRAF-APA measurements in late stages of RCD when NIRAF-APA limits become ill defined (e.g., in patient CIC03005) (Fig. 1C). This may explain some discrepancies between observed EZ and NIRAF-APA parameters. Previously published OCT data in *CLRN1*-*USH3A* patients²⁹ documented the progression of retinal thinning with age. Our study takes into account the EZ diameter, as it probably correlated better with the functional parameters.^{35,36} The loss of outer retinal layers on SD-OCT was in line with SWAF and NIRAF findings (e.g., $-76 \mu\text{m}/\text{y}$ on average for CIC02644). All of our patients had cystic macular changes in the course of our monitoring.

Of note, we found an unusual phenotype of *CLRN1* RCD consisting of a whitish granularity of the midperipheral retina giving a spotted marbled appearance that was present in all four patients. This finding was correlated with the presence of numerous hyperreflective dots in the subretinal space on SD-OCT, especially in patients with prominent whitishness of the retina (Figs. 1B, 1C; Supplementary Fig. 1). We hypothesize that it might be debris of degenerating photoreceptors and/or retinal pigment epithelium. Alternatively, we cannot exclude the possibility that the whitishness

could be a general feature of RCD at this time point. Indeed, our study involved patients of nearly the same age. This finding was not reported in the description of the Finnish or Ashkenazi Jewish cohorts^{25,26,29} or evident on published fundus photographs.^{30,39}

Patients CIC03005 and CIC05477, both from Ivory Coast ancestry and harboring the same homozygous variant c.368C>A, p.(Ala123Asp), were initially assessed by the end of their 20s. Foveal EZ and RPE were already disorganized in CIC03005 at 17 years of age, whereas there was a well-preserved foveal island of outer retina in CIC05477 at 19 years of age. These data suggest some phenotypic variability in *CLRN1*-related RCD, also common for other inherited retinal disorders.²⁸ This pathogenic variant was first reported in a French Canadian patient.³⁵ The retinal phenotype of this patient has not been published. Patients CIC03005 and CIC05477 did not report any common ancestor and were born in different Ivory Coast districts; however, a founder effect cannot be excluded considering an enrichment of this allele in the French Light4Deaf cohort.

The gene coding for clarin-1, *CLRN1*, is a four exon gene located on chromosome 3q25.1.^{27,40} Multiple transcripts have been reported for this gene,⁴⁰ but the major mRNA transcript variant, comprised of exons 0, 2, and 3 (RefSeq NM_174878.3), is expressed in the retina⁴¹ and encodes a protein of 232 amino acid residues (clarin-1 isoform a). A minor mRNA transcript, comprised of exons 1, 2, 3a, and 3b (RefSeq NM_052995.2), encodes a protein of 120 amino acid residues (clarin-1 isoform c). Clarin-1 is a small transmembrane protein belonging to the tetraspanin and claudin families. A major retinal isoform a is predicted to be comprised of four transmembrane domains and is glycosylated at Asn48 residue.¹⁷ Multiple sequence alignment algorithms have depicted a close similarity of clarin-1 with the voltage-dependent calcium channel gamma-2 subunit, *CACNG2* (MIM #602911), also known as stargazin.¹⁷ The putative function of clarin-1 in cells was deduced from this resemblance. Adato and colleagues¹⁷ speculated that clarin-1 may have a role in the structure and function of the ribbon synapse and in protein-protein bridging in the synaptic cleft. The protein is localized ubiquitously with higher levels in the spiral ganglion cells of the inner ear, in the olfactory epithelium, in the testis and in the retina. RNA in situ hybridization and single-cell RNA sequencing demonstrated the localization of mRNA transcripts in the inner nuclear layer and more precisely in the Müller cells for both mouse and human retinas.⁴²

The mechanism of *CLRN1*-related RCD remains unknown because there is no mouse model of clarin-1-associated RCD: knock-in and knock-out mice for *Clrn1* do not produce any detectable retinal disease.^{42,43} Plausible hypotheses for the discrepancy between human and mouse phenotypes have been formulated. First, it is possible that *CLRN1* expression does not follow the same spatial and temporal pattern across mammalian species. For example, there is a developmental downregulation of *Clrn1* expression in mouse retina and not in human.^{42,43} The absence of well-developed, actin-filled calyceal processes at the apical region of inner segments of mouse photoreceptors represents a second possibility.⁴⁴ As the Usher syndromes are a part of the ciliopathy spectrum, clarin-1 could take part in the structure or/and function of the photoreceptor connecting cilium; unfortunately, limited experimental data are available to support this hypothesis. A better understanding of the retinal localization and function of clarin-1 would be crucial for

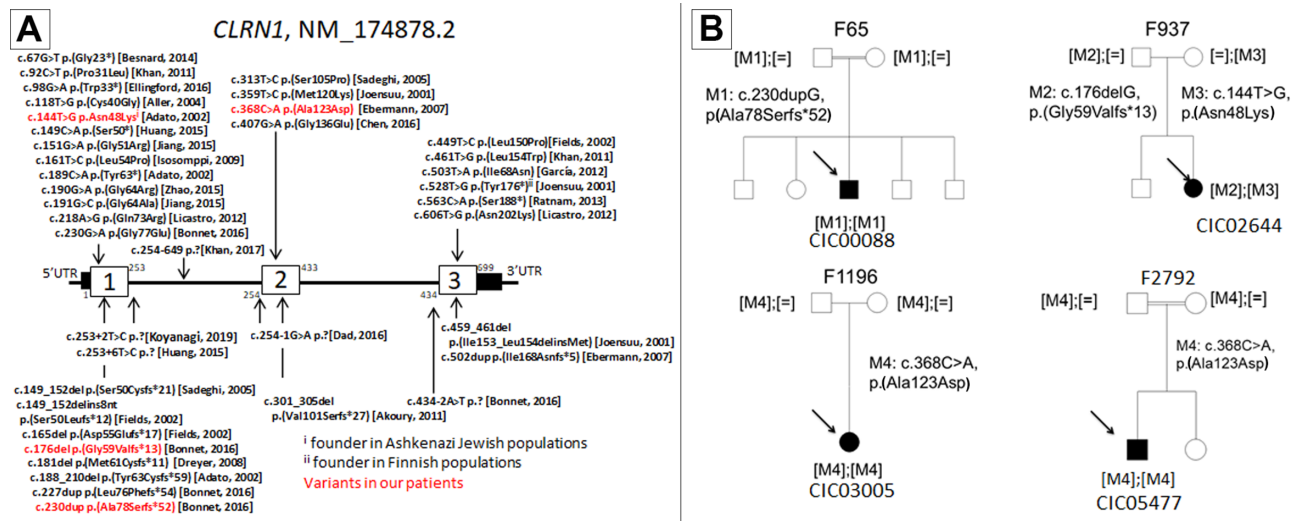


FIGURE 3. Pedigrees and variants in *CLRN1*. (A) Pathogenic variants are drawn in major retinal transcript coding for clarin-1 isoform a. Variants found in our cohort are shown in red. (B) Pedigrees. Two probands (F65, CIC00088; F2792, CIC05477) reported parental consanguinity. Both cases with the c.368C>A, p.(Ala123Asp) variant were from Ivory Coast ancestry.

translational research, such as developing gene replacement protocols, as *CLRN1* is a small gene, suitable for viral delivery, unlike other USH-related genes.⁴⁵

In contrast, the inner ear dysfunction phenotype could be obtained and rescued in mutant mice. Clarin-1 is essential for the morphogenesis and maintenance of the stereocilia hair bundle in auditory hair cells.⁴⁶ At the molecular level, the protein is supposed to be necessary for the regulation of actin cytoskeleton and of the F-actin core of the stereocilia hair cell.^{47,48} The stereocilia in *Clrn1* knock-out mice are poorly developed and disorganized.^{43,49} Viral-based gene augmentation therapy prevents early-onset deafness and limits the progression of SNHL in this model.⁴⁸

Two founder pathogenic variants have been reported and account for most cases: c.528T>G, p.(Tyr176*) in the Finnish population³² and c.144T>G, p.(Asn48Lys) in Ashkenazi Jews.¹⁷ Thirty-eight other disease-causing variants in *CLRN1* (Fig. 3A) have been reported to date (<http://www.hgmd.cf.ac.uk/>; <https://databases.lovd.nl/shared/variants/CLRN1/unique>), with missense and nonsense pathogenic variants being the most frequent.²⁴

Some genotype–phenotype associations related to *CLRN1* variants have been described. Amino acid changes found in the intra- and extracellular loops are thought to be more damaging than non-polar amino acid substitutions within the transmembrane domains that could give rise to non-syndromic RP61.¹⁹ As our patients were selected on the basis of their clinical phenotype and their number was small, we cannot come to conclusions. Larger cohorts of patients in collaborative projects would be necessary to explore genotype–phenotype correlations.

In summary, we have described relatively severe and rapidly progressive *CLRN1*-associated RCD with a distinctive retinal granularity and whitishness not previously reported (Fig. 1, Supplementary Fig. S1). It accounts for 1.4% of the cases in our large French USH cohort. Although the variants in *CLRN1* harbored by our patients have already been reported, the associated ocular phenotype has not.

Acknowledgments

The authors are grateful to Katia Marazova (Institut de la Vision, Paris, France) for her English revisions. The authors thank families participating in the study and the clinical staff from the National Center for Rare Diseases REFERET. DNA samples were obtained from the NeuroSensCol DNA bank, for research in neuroscience (PI, J.-A.S.; co-PI, I.A.; partner with CHNO des Quinze-Vingts, Inserm, and CNRS, certified NFS96-900).

Supported by funding from RHU-Light4deaf (ANR-15-RHU-0001) and LABEX LIFESENSES (ANR-10-LABX-65); French state funds managed by the Agence Nationale de la Recherche within the Investissements d’Avenir program (ANR-21-11-IDEX-0004-0); IHU FOReSIGHT (ANR-18-IAHU-0001), which is supported by French state funds managed by the Agence Nationale de la Recherche within the Investissements d’Avenir program; and Foundation Fighting Blindness center grant (C-CMM-0907-0428-INSERM04). The funding organizations had no role in the design or conduct of this research.

Presented as Poster #3033 (abstract #3362510) at ARVO 2020 (online).

Disclosure: V.M. Smirnov, None; M. Nassisi, None; S. Mohand-Saïd, None; C. Bonnet, None; A. Auboïs, None; C. Devisme, None; T. Dib, None; C. Zeitz, None; N. Loundon, None; S. Marlin, None; C. Petit, None; B. Bodaghi, None; J.-A. Sahel, None; I. Audo, None

References

- Boughman JA, Vernon M, Shaver KA. Usher syndrome: definition and estimate of prevalence from two high-risk populations. *J Chronic Dis*. 1983;36(8):595–603.
- Hartong DT, Berson EL, Dryja TP. Retinitis pigmentosa. *Lancet*. 2006;368(9549):1795–1809.
- Keats BJ, Corey DP. The usher syndromes. *Am J Med Genet*. 1999;89(3):158–166.
- Kimberling WJ, Hildebrand MS, Shearer AE, et al. Frequency of Usher syndrome in two pediatric populations: implications for genetic screening of deaf and hard of hearing children. *Genet Med*. 2010;12(8):512–516.

5. Mathur PD, Yang J. Usher syndrome and non-syndromic deafness: functions of different whirlin isoforms in the cochlea, vestibular organs, and retina. *Hear Res.* 2019;375:14–24.
6. Heissler SM, Manstein DJ. Functional characterization of the human myosin-7a motor domain. *Cell Mol Life Sci.* 2012;69(2):299–311.
7. Weil D, Blanchard S, Kaplan J, et al. Defective myosin VIIA gene responsible for Usher syndrome type 1B. *Nature.* 1995;374(6517):60–61.
8. Bonnet C, El-Amraoui A. Usher syndrome (sensorineural deafness and retinitis pigmentosa): pathogenesis, molecular diagnosis and therapeutic approaches. *Curr Opin Neurol.* 2012;25(1):42–49.
9. Bhattacharya G, Kalluri R, Orten DJ, Kimberling WJ, Cosgrove D. A domain-specific usherin/collagen IV interaction may be required for stable integration into the basement membrane superstructure. *J Cell Sci.* 2004;117(2):233–242.
10. Eudy JD, Weston MD, Yao S, et al. Mutation of a gene encoding a protein with extracellular matrix motifs in Usher syndrome type IIa. *Science.* 1998;280(5370):1753–1757.
11. Seyedahmadi BJ, Rivolta C, Keene JA, Berson EL, Dryja TP. Comprehensive screening of the *USH2A* gene in Usher syndrome type II and non-syndromic recessive retinitis pigmentosa. *Exp Eye Res.* 2004;79(2):167–173.
12. Ávila-Fernández A, Cantalapiedra D, Aller E, et al. Mutation analysis of 272 Spanish families affected by autosomal recessive retinitis pigmentosa using a genotyping microarray. *Mol Vis.* 2010;16:2550–2558.
13. McGee TL, Seyedahmadi BJ, Sweeney MO, Dryja TP, Berson EL. Novel mutations in the long isoform of the *USH2A* gene in patients with Usher syndrome type II or non-syndromic retinitis pigmentosa. *J Med Genet.* 2010;47(7):499–506.
14. Nuutila A. Dystrophia retinae pigmentosa–dysacusis syndrome (DRD): a study of the Usher- or Hallgren syndrome. *J Genet Hum.* 1970;18(1):57–88.
15. Gorlin RJ, Tilsner TJ, Feinstein S, Duvall AJ. Usher's syndrome type III. *Arch Otolaryngol Chic Ill 1960.* 1979;105(6):353–354.
16. Sadeghi M, Cohn ES, Kimberling WJ, Tranebjaerg L, Möller C. Audiological and vestibular features in affected subjects with *USH3*: a genotype/phenotype correlation. *Int J Audiol.* 2005;44(5):307–316.
17. Adato A, Vreugde S, Joensuu T, et al. *USH3A* transcripts encode clarin-1, a four-transmembrane-domain protein with a possible role in sensory synapses. *Eur J Hum Genet.* 2002;10(6):339–350.
18. Abbott JA, Meyer-Schuman R, Lupo V, et al. Substrate interaction defects in histidyl-tRNA synthetase linked to dominant axonal peripheral neuropathy. *Hum Mutat.* 2018;39(3):415–432.
19. Khan MI, Kersten FFJ, Azam M, et al. *CLRN1* mutations cause nonsyndromic retinitis pigmentosa. *Ophthalmology.* 2011 Jul 1;118(7):1444–1448.
20. Puffenberger EG, Jinks RN, Sougnez C, et al. Genetic mapping and exome sequencing identify variants associated with five novel diseases. *PLoS One.* 2012;7(1):e28936.
21. Vester A, Velez-Ruiz G, McLaughlin HM, et al. A loss-of-function variant in the human histidyl-tRNA synthetase (*HARS*) gene is neurotoxic in vivo. *Hum Mutat.* 2013;34(1):191–199.
22. Safka Brozkova D, Deconinck T, Griffin LB, et al. Loss of function mutations in *HARS* cause a spectrum of inherited peripheral neuropathies. *Brain J Neurol.* 2015;138(Pt 8):2161–2172.
23. Galatolo D, Kuo ME, Mullen P, et al. Bi-allelic mutations in *HARS1* severely impair histidyl-tRNA synthetase expression and enzymatic activity causing a novel multisystem ataxic syndrome. *Hum Mutat.* 2020;41(7):1232–1237.
24. Bonnet C, Riahi Z, Chantot-Bastarud S, et al. An innovative strategy for the molecular diagnosis of Usher syndrome identifies causal biallelic mutations in 93% of European patients. *Eur J Hum Genet.* 2016;24(12):1730–1738.
25. Pakarinen L, Tuppurainen K, Laippala P, Mäntyjärvi M, Puhakka H. The ophthalmological course of Usher syndrome type III. *Int Ophthalmol.* 1995;19(5):307–311.
26. Khalailah A, Abu-Diab A, Ben-Yosef T, et al. The genetics of Usher syndrome in the Israeli and Palestinian populations. *Invest Ophthalmol Vis Sci.* 2018;59(2):1095–1104.
27. Fields RR, Zhou G, Huang D, et al. Usher syndrome type III: revised genomic structure of the *USH3* gene and identification of novel mutations. *Am J Hum Genet.* 2002;71(3):607–617.
28. Ness SL, Ben-Yosef T, Bar-Lev A, et al. Genetic homogeneity and phenotypic variability among Ashkenazi Jews with Usher syndrome type III. *J Med Genet.* 2003;40(10):767–772.
29. Herrera W, Aleman TS, Cideciyan AV, et al. Retinal disease in Usher syndrome III caused by mutations in the *clarin-1* gene. *Invest Ophthalmol Vis Sci.* 2008;49(6):2651.
30. Ratnam K, Västinsalo H, Roorda A, Sankila E-MK, Duncan JL. Cone structure in patients with usher syndrome type III and mutations in the *Clarin 1* gene. *JAMA Ophthalmol.* 2013;131(1):67–74.
31. Audo I, Friedrich A, Mohand-Said S, Lancelot M-E, Antonio A, Moskova-Doumanova V, Poch O, Bhattacharya S, Sahel J-A, Zeit C. An unusual retinal phenotype associated with a novel mutation in *RHO*. *Arch Ophthalmol.* 2010;128(8):1036–1045.
32. Joensuu T, Hämäläinen R, Yuan B, et al. Mutations in a novel gene with transmembrane domains underlie Usher syndrome type 3. *Am J Hum Genet.* 2001;69(4):673–684.
33. Ebermann I, Lopez I, Bitner-Glindzic M, Brown C, Koenekoop RK, Bolz HJ. Deafblindness in French Canadians from Quebec: a predominant founder mutation in the *USH1C* gene provides the first genetic link with the Acadian population. *Genome Biol.* 2007;8(4):R47.
34. Richards S, Aziz N, Bale S, et al. Standards and guidelines for the interpretation of sequence variants: a joint consensus recommendation of the American College of Medical Genetics and Genomics and the Association for Molecular Pathology. *Genet Med.* 2015;17(5):405–424.
35. Pakarinen L, Karjalainen S, Simola KOJ, Laippala P, Kaitalo H. Usher's syndrome type 3 in Finland. *Laryngoscope.* 1995;105(6):613–617.
36. Plantinga RF, Pennings RJE, Huygen PLM, et al. Visual impairment in Finnish Usher syndrome type III. *Acta Ophthalmol Scand.* 2006;84(1):36–41.
37. Duncker T, Tabacaru MR, Lee W, Tsang SH, Sparrow JR, Greenstein VC. Comparison of near-infrared and short-wavelength autofluorescence in retinitis pigmentosa. *Invest Ophthalmol Vis Sci.* 2013;54(1):585–591.
38. Nassisi M, Lavia C, Mohand-Said S, et al. Near-infrared fundus autofluorescence alterations correlate with swept-source optical coherence tomography angiography findings in patients with retinitis pigmentosa. *Sci Rep.* 2021;11(1):3180.
39. Ebermann I, Wilke R, Lauhoff T, Lübben D, Zrenner E, Bolz HJ. Two truncating *USH3A* mutations, including one novel, in a German family with Usher syndrome. *Mol Vis.* 2007;13:1539–1547.
40. Västinsalo H, Jalkanen R, Dinculescu A, et al. Alternative splice variants of the *USH3A* gene *Clarin 1* (*CLRN1*). *Eur J Hum Genet.* 2011;19(1):30–35.
41. Zallochi M, Meehan DT, Delimont D, et al. Localization and expression of *clarin-1*, the *Clrn1* gene product, in auditory hair cells and photoreceptors. *Hear Res.* 2009;255(1–2):109–120.

42. Xu L, Bolch SN, Santiago CP, et al. *Clarin-1* expression in adult mouse and human retina highlights a role of Müller glia in Usher syndrome. *J Pathol.* 2020;250(2):195–204.
43. Geller SF, Guerin KI, Visel M, et al. CLRN1 is nonessential in the mouse retina but is required for cochlear hair cell development. *PLoS Genet*;5(8):e1000607.
44. Sahly I, Dufour E, Schietroma C, et al. Localization of Usher 1 proteins to the photoreceptor calyceal processes, which are absent from mice. *J Cell Biol.* 2012;199(2):381–399.
45. Dinculescu A, Stupay RM, Deng W-T, et al. AAV-mediated clarin-1 expression in the mouse retina: implications for USH3A gene therapy. *PLoS One.* 2016;11(2):e0148874.
46. Geng R, Melki S, Chen DH-C, et al. The mechanosensory structure of the hair cell requires clarin-1, a protein encoded by Usher syndrome III causative gene. *J Neurosci.* 2012;32(28):9485–9498.
47. Tian G, Zhou Y, Hajkova D, et al. Clarin-1, encoded by the Usher syndrome III causative gene, forms a membranous microdomain: possible role of clarin-1 in organizing the actin cytoskeleton. *J Biol Chem.* 2009;284(28):18980–18993.
48. Geng R, Omar A, Gopal SR, et al. Modeling and preventing progressive hearing loss in Usher syndrome III. *Sci Rep.* 2017;7(1):13480.
49. Geng R, Geller SF, Hayashi T, et al. Usher syndrome IIIA gene clarin-1 is essential for hair cell function and associated neural activation. *Hum Mol Genet.* 2009;18(15):2748–2760.